# Aqueous Electrochemistry of Mono- and Bi-nuclear Copper(II) Complexes with Polyaza[*n*]paracyclophane Ligands

**Antonio Doménech,[a] José-Vicente Folgado,[a] Enrique García-España,[a] Santiago V. Luis,[b] José-M. Llinares,[a] Juan F. Miravet[b] and José A. Ramírez[a]**

[a] *Department of Inorganic Chemistry, University of Valencia, 46100 Burjassot (Valencia), Spain*

[b] *Laboratory of Organic Chemistry, Department of Experimental Sciences, University Jaume I, 12080 Castellón, Spain*

The aqueous electrochemistry of the $Cu^{2+}$ complexes of the azaparacyclophanes 2,6,9,13-tetraaza[14]paracyclophane ($L^1$), 2,5,8,11-tetraaza[12]paracyclophane ($L^2$) and 2,5,8,11,14-pentaaza[15]paracyclophane ($L^3$) has been studied. Copper(II) forms stable mononuclear $[CuH_rL]^{(2+r)+}$ species with all three ligands ($r = -1$ to 1, $L^1$ and $L^2$; $-1$ to 2, $L^3$) while $L^2$ and $L^3$ also form binuclear $[Cu_2H_rL]^{(4+r)+}$ species ($r = -2$, $L^2$; 0 to $-2$, $L^3$) in a pH-dependent stepwise manner. Frozen-solution ESR measurements show that all the complexes prefer a square-planar co-ordination. In neutral and basic media reduction at mercury and glassy carbon electrodes occurs in two quasi-reversible steps, indicating the formation of stable $Cu^+$ species. Stabilization of the $Cu^+$ complexes with respect to disproportionation in the order $L^3 > L^1 > L^2$ has been found.

The electrochemistry of copper complexes has attracted a great deal of interest because of the biological significance of the $Cu^{2+}$–$Cu^+$ couple. The ready accessibility of the $Cu^+$ oxidation state is at the origin of the function of copper electron-transfer proteins as well as the mechanisms of copper enzymes.[1] Therefore, over the last two decades intensive investigations have been carried out on the generation of copper complexes with macrocyclic ligands in order to achieve a better understanding of the chemistry of metallobiomolecules.[2] Several thiaazamacrocycles have been revealed as particularly interesting probes for this purpose.[3,4]

The majority of $Cu^{2+}$ complexes of azamacrocycles studied reduce at mercury electrodes in a single two-electron step. However, it has recently been reported that $Cu^+$ complexes can be stabilized by N-permethylation of saturated azamacrocycles. For instance, N-permethylation of the macrocycle 5,5,7,12,12,14-hexamethyl-1,4,8,11-tetraazacyclotetradecane ($L^4$) to give $L^5$ largely stabilizes $Cu^+$ in aqueous solution even when exposed to air.[5] Similar results were also obtained with the N-permethylated open-chain polyamine 2,5,9,12-tetramethyl-2,5,9,12-tetraazatridecane ($L^6$) which reduces $Cu^{2+}$ in two successive one-electron steps, indicating the formation of a stable $Cu^+$ complex.[6]

This behaviour has been explained mainly in terms of the hydrophobicity of the molecule induced by permethylation of the nitrogen atoms, although some other factors like stereochemical hindrance and the poorer σ-donor character of the tertiary nitrogens in aqueous solution could not be discarded.

We have recently synthesized[7,8] a series of azaparacyclophanes containing a single *para*-substituted benzene spacer interrupting saturated polyamine bridges of different lengths and numbers of nitrogen atoms. 2,6,9,13-Tetraaza[14]paracyclophane ($L^1$), 2,5,8,11-tetraaza[12]paracyclophane ($L^2$) and 2,5,8,11,14-pentaaza[15]paracyclophane ($L^3$) are representatives of this series of receptors. We observed that the *p*-benzene moiety prevents the simultaneous co-ordination of all nitrogen sites to the metal centre producing a drop in the stability of these complexes when compared to those of analogous saturated macrocycles. Therefore, a maximum of three of the nitrogen atoms in the macrocycle would be co-ordinating the metal ion, the co-ordination being completed by water molecules of the solvent. This situation is clearly reflected by the crystal structure of the binuclear complex $[Cu_2L^2Cl_4]\cdot 1.5H_2O$ in which it can be seen how the benzene moiety organizes the ligand into two ethylenediamine subunits.[8] The co-ordination sphere around each $Cu^{2+}$ ion is completed by two chloride ions in the plane with one other at a much greater distance to give an axially elongated square-pyramidal geometry. The aromatic spacer, on the other hand, should also increase the hydrophobicity of the molecule.

All of these considerations make these ligands suitable candidates for studying their chemical behaviour towards either $Cu^+$ stabilization or avoiding $Cu^+$ disproportionation into $Cu^{2+}$ and $Cu^0$.

In the present paper we report a cyclic voltammetric and coulometric study of the aqueous electrochemistry of copper compounds of ligands $L^1$–$L^3$, revealing that $Cu^+$ species stable towards disproportionation are formed in alkaline aqueous media. The electrochemical behaviour of mono- and bi-nuclear copper complexes of these azaparacyclophanes is also compared with that of related saturated polyazaalkanes.

## Experimental

All electrochemical experiments were carried out in a three-electrode cell thermostatted at 298 K under an atmosphere of argon. Cyclic voltammograms were obtained with a potentiostat (AR 100), a signal generator (Newtronic 200P) and an *x*–*y* recorder (Riken-Denshi F35). A glassy carbon electrode (GCE) (0.071 $cm^2$) and a hanging mercury drop electrode (HMDE) (Metrohm AGCH9100) were used as working electrodes. A platinum-wire auxiliary electrode and a saturated calomel reference electrode (SCE) completed the three-electrode arrangement. Solid working electrodes were cleaned and activated prior to a series of runs. Electrochemical pretreatment of the GCE was performed in 0.10 mol $dm^{-3}$ potassium nitrate by applying 1.75 V *vs.* SCE for 5 min followed by $-1.0$ V for 1 min.[9]

For the coulometric experiments, a mercury pool was used and the auxiliary electrode was filled with solvent and supporting electrolyte only in a compartment isolated from the bulk solution by a fine-porosity frit. Controlled-potential electrolyses were conducted at potentials slightly more negative

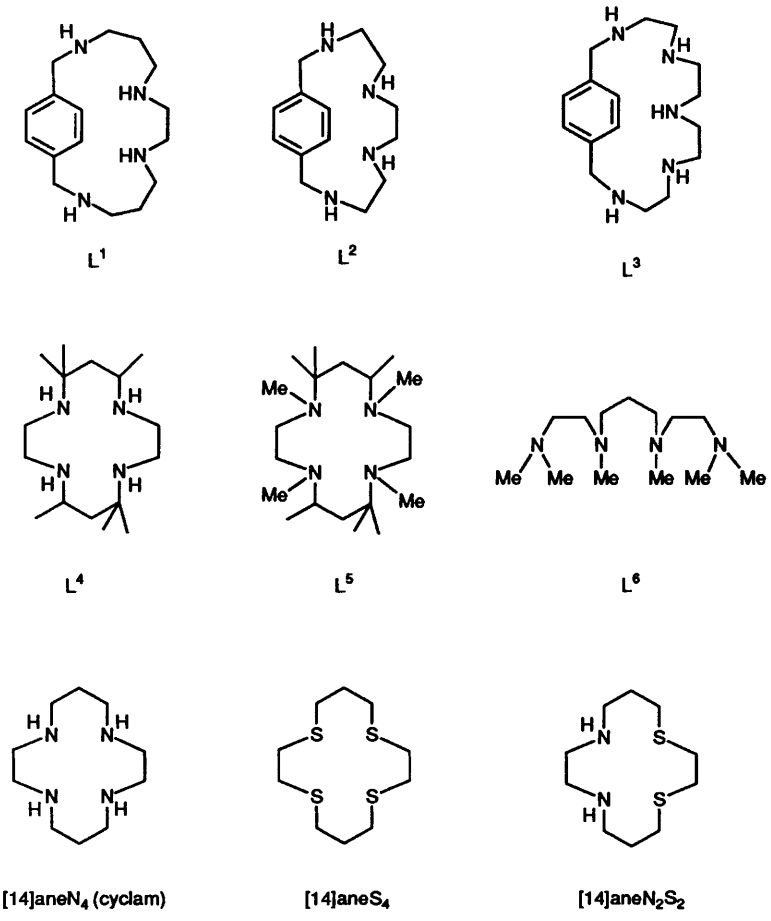


than the observed reductions under identical conditions to those used for cyclic voltammetry. Potentiostatic chronoamperograms and coulometries were monitored on a *y–t* recorder (JJ CR550).

Electrochemical experiments were performed in solutions of $Cu(ClO_4)_2 \cdot 2H_2O$ (Merck) in doubly distilled water. Ligands were prepared and purified as previously described.[7] Either $NaClO_4$ (0.15 mol $dm^{-3}$) or $NEt_4ClO_4$ (0.15 mol $dm^{-3}$) was used as the supporting electrolyte. The pH was adjusted to the required value by addition of appropriate amounts of $HClO_4$ and/or NaOH and controlled before and after each run.

Potentiometric constants of the ligands $L^1$–$L^3$* and formation constants of the copper(II) complexes were taken from refs. 7 and 8. The program SUPERQUAD,[10] based on a non-linear regression fit with variable statistical weighting, was used to calculate the stability and protonation constants. The ionic product of water under our experimental conditions was $pK_w = 13.73(1)$.

Proton and $^{13}C$ NMR spectra were recorded on Varian UNITY 300 and 400 spectrometers operating at 299.95 and 399.95 MHz for $^1H$ and 75.43 and 100.68 MHz for $^{13}C$. For the $^{13}C$ NMR spectra dioxane was used as the standard reference (δ 67.4) and for the $^1H$ spectra the solvent signal. X-Band (9.45 GHz) ESR spectra of frozen solutions at 130 K were recorded with a Bruker ER 200D spectrometer equipped with a low-temperature control unit and using diphenylpicrylhydrazyl ($g = 2.0036$) as reference.

* Stepwise protonation constants for the ligands $L^1$–$L^3$, determined in 0.15 mol $dm^{-3}$ $NaClO_4$ at 298.1 K, taken from refs. 7 and 8 are: $L^1$ log $K_{HL} = 9.93(1)$, log $K_{H_2L} = 9.09(1)$, log $K_{H_3L} = 7.44(1)$, log $K_{H_4L} = 3.61(1)$; $L^2$ log $K_{HL} = 9.39(2)$, log $K_{H_2L} = 8.45(2)$, log $K_{H_3L} = 5.38(2)$, log $K_{H_4L} = 2.51(1)$; $L^3$ log $K_{HL} = 10.68(2)$, log $K_{H_2L} = 9.29(1)$, log $K_{H_3L} = 8.66(2)$, log $K_{H_4L} = 7.23(2)$, log $K_{H_5L} = 3.93(2)$.

## Results and Discussion

*Electrochemical Data.*—The electrochemical properties of the complexes were studied by cyclic voltammetry throughout the pH range 3–11. Below pH 4.5, cyclic voltammograms of uncomplexed $Cu^{2+}$ solutions at the HMDE exhibit a two-electron reversible couple [see Fig. 1(*a*)] (AA′) whose formal potential varies with $Cu^{2+}$ concentration according to the Nernst equation for the $Cu^{2+}$–Cu(amalgam) couple ($E° = 95$ mV *vs.* SCE). As shown in Fig. 2(*a*), the cyclic voltammogram at the CGE shows a cathodic peak (A) followed by a prominent anodic signal (A′) attributable to the formation of a metallic film over the electrode surface during the prior reduction step.

In the presence of the receptors $L^1$, $L^2$ and $L^3$ the cyclic voltammetric pattern is significantly altered depending on the pH and the ligand to metal molar ratio, L:M. Substitution of $NEt_4ClO_4$ by $NaClO_4$ as a supporting electrolyte led to identical cyclic voltammetric responses, indicating no influence of the excess of $Na^+$ on the electrochemical mechanism and stability constants.

Addition of receptor to weakly acidic solutions results in a cathodic shift of the AA′ couple, accompanied by the appearance of a second cathodic peak [Fig. 1(*b*)], X, in the HMDE voltammograms. The electrochemical parameters for the AA′ couple indicate that wave A can be assigned to the reduction of $Cu^{2+}$ ions preceded by the dissociation of the complex. This mechanism parallels that described for complexes of transition metals with organic ligands containing amino groups.[11] Thus, the overall electrode process can be described by equation (1).†

$$[Cu^{II}H_rL] + 2e^- \longrightarrow Cu^0 + H_rL \quad (1)$$

† Charges in the complexed species have been omitted for clarity.

The second wave can be described as a two-electron proton-assisted reduction of the complex species [equation (2)].

$$[Cu^{II}H_rL] + H^+ + 2e^- \longrightarrow Cu^0 + H_{r+1}L \quad (2)$$

Because there is no anodic counterpart of wave X, reduction of the complex must involve an irreversible electron transfer while peak A' corresponds to the oxidation of the copper amalgam formed during the prior reduction processes. By increasing the sweep rate the peak current of wave A decreases and its peak potential shifts in the anodic direction. Conversely, the peak current of wave X increases as the scan rate increases whereas its peak potential is displaced in the cathodic direction. Finally, as the scan rate is increased the potential of wave A' shifts to more anodic values and follows the potential of peak A. These results are as expected according to the proposed mechanism.

In neutral and basic media, however, the electrochemical response changes drastically. As shown in Fig. 1(*c*), the cyclic voltammograms exhibit two quasi-reversible couples (BB' and CC'). The peak to half-peak potential separation ($E_p - E_{p/2}$ = 60 mV), the value of the individual peak functions ($I_p = i_p/Acv^{\frac{1}{2}}$ = 500–600 A cm mol$^{-1}$ V$^{-\frac{1}{2}}$ s$^{\frac{1}{2}}$ where $A$ = electrode area in cm$^2$ and $c$ = bulk concentration in mol dm$^{-3}$) and the linear dependence of the peak current with the square root of the scan rate indicate that both these processes are one-electron reversible diffusion-controlled electrode reactions.[12] The cyclic voltammetric pattern remains unchanged when the scan rate is varied indicating that no coupled chemical reactions occur. The electrochemical processes B and C can be represented by equations (3) and (4), indicating stabilization of the $Cu^+$

$$[Cu^{II}H_rL] + e^- \longrightarrow [Cu^{I}H_rL] \quad (3)$$

$$[Cu^{I}H_rL] + e^- \longrightarrow Cu^0 + H_rL \quad (4)$$

oxidation state with respect to disproportionation by the effect of co-ordination to the macrocyclic receptors. The electrochemical parameters summarized in Table 1 agree with the previous assignments for the electrode processes. Similar features were observed at the GCE. In weakly acidic solutions, a cathodic shift of the potentials accompanied by a decrease of the peak currents takes place. As shown in Fig. 2(*b*), peak A' vanishes and is replaced by overlapping oxidation peaks B'C' at more negative potentials. In neutral and alkaline media, the cathodic portions of the cyclic voltammograms exhibit two strongly overlapping peaks B and C [see Fig. 2(*c*)] whose anodic counterparts resemble single oxidation peaks.

The pH dependence of the electrochemical parameters agrees well with the distribution diagram calculated from potentiometric data. Variation of peak potentials with pH for the Cu–L[1] system, depicted in Fig. 3, clearly reveals the existence of two well defined pH zones: in acidic media, no complexation occurs and the electrochemical response is that displayed for free copper solutions; in weakly acidic, neutral and alkaline media, $Cu^+$ complexes are stabilized with respect to disproportionation and reduction at the electrode surface takes place in two consecutive steps.

The cyclic voltammetric response for the Cu–L[2] and the Cu–L[3] systems for L:M $\geqslant$ 1 is quite similar to that described above. For molar ratios close to 0.5, binuclear species predominate in the alkaline region. Then, the cyclic voltammograms consist of two one-electron almost reversible couples BB' and CC'. The peak potentials are displaced, however, with respect those recorded for L:M > 1 at the same pH. In fact, for L:M ratios close to 0.8, the cyclic voltammograms become more complex and resemble the superposition of four couples indicating the coexistence of

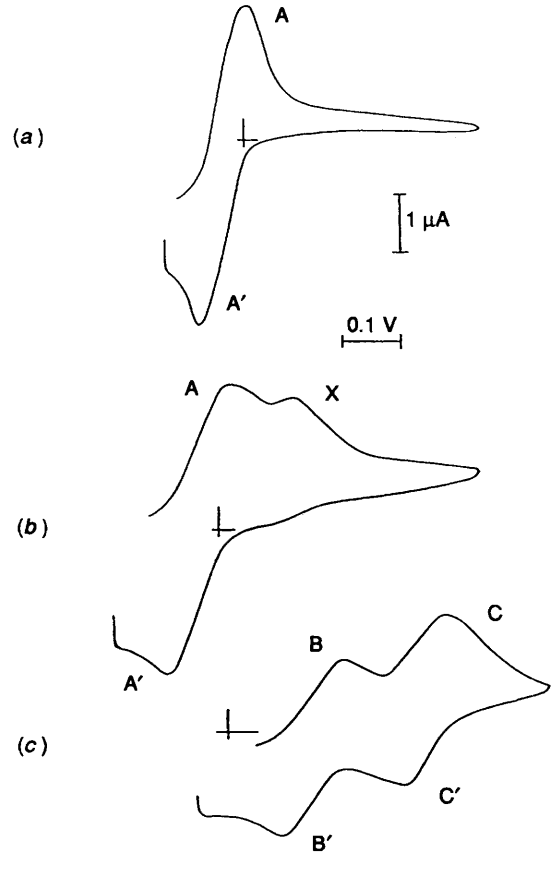


**Fig. 1** Cyclic voltammograms for solutions of (*a*) $Cu(ClO_4)_2 \cdot 2H_2O$ at pH 4.0; (*b*) $Cu(ClO_4)_2$ and L[1] at pH 4.50; (*c*) $Cu(ClO_4)_2 \cdot 2H_2O$ and L[1] at pH 8.50. All concentrations 0.80 × 10$^{-3}$ mol dm$^{-3}$; HMDE, scan rate 0.05 V s$^{-1}$, 0.15 mol dm$^{-3}$ $NaClO_4$

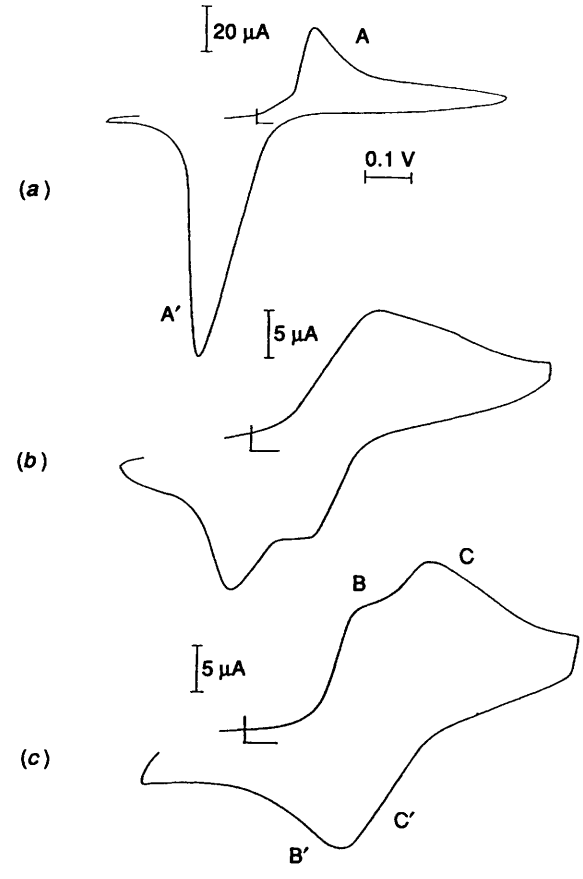


**Fig. 2** (*a*) Cyclic voltammogram at the GCE for a $Cu(ClO_4)_2 \cdot 2H_2O$ solution (1.0 × 10$^{-3}$ mol dm$^{-3}$) at pH 4.00; scan rate 0.20 V s$^{-1}$. Cyclic voltammograms upon addition of L[1] (1.0 × 10$^{-3}$ mol dm$^{-3}$) at (*b*) pH 6.0 and (*c*) pH 9.0. Supporting electrolyte 0.15 mol dm$^{-3}$ $NaClO_4$

**Table 1** Electrochemical parameters recorded at the HMDE for scan rates in the range 0.05–0.50 V $s^{-1}$ in 0.15 mol $dm^{-3}$ $NaClO_4$ at 298.1 K. All solutions were 0.50 × $10^{-3}$ mol $dm^{-3}$ in electroactive species. Formal potentials (± 5 mV) at the HMDE in mV *vs.* SCE. Current functions in A cm $mol^{-1}$ $V^{-\frac{1}{2}}$ $s^{\frac{1}{2}}$ for the cathodic process at the HMDE. The uncertainty in the current function was estimated as 5% of the tabulated values

| Species | pH | $E^{0\prime}$ (BB′) | $I_{pc}$ | $E^{0\prime}$ (CC′) | $I_{pc}$ |
|---|---|---|---|---|---|
| $[Cu(HL^1)]$ | 7.20 | −150 | 600 | −310 | 600 |
| $[CuL^1]$ | 8.35 | −150 | 600 | −315 | 650 |
| $[CuL^1(OH)]$ | 8.80 | −150 | 570 | −315 | 550 |
| $[CuL^2]$ | 9.20 | −180 | 600 | −245 | 550 |
| $[CuL^2(OH)]$ | 10.35 | −195 | 550 | −250 | 550 |
| $[Cu_2L^2(OH)_2]$ | 10.25 | −185 | 1200 | −250 | 1000 |
| $[Cu(H_2L^3)]$ | 6.40 | −135 | 600 | −320 | 650 |
| $[Cu(HL^3)]$ | 8.30 | −155 | 650 | −325 | 600 |
| $[CuL^3]$ | 9.80 | −170 | 600 | −340 | 550 |
| $[Cu_2L^3(OH)]$ | 9.50 | −205 | 1000 | −400 | 1100 |
| $[Cu_2L^3(OH)_2]$ | 10.40 | −215 | 1100 | −415 | 1100 |

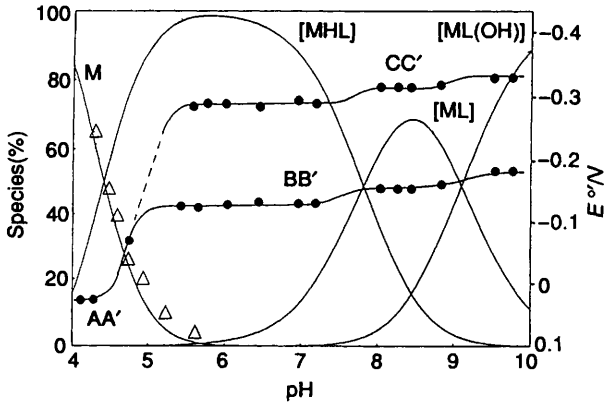


**Fig. 3** Comparison of the pH dependence of the formal potentials (calculated as the half-sum of the voltammetric peak potentials) at the HMDE for the Cu–$L^1$ system with the distribution diagram calculated from potentiometric data; $c_M = c_L = 1.0 \times 10^{-3}$ mol $dm^{-3}$

mono- and bi-nuclear complex species, as shown by the potentiometric data. It was observed that on increasing the L : M ratio the peaks corresponding to the mononuclear species progressively replace the peaks for the binuclear species until their complete disappearance at L : M ratios of *ca.* 1.5.

The waves of the binuclear species appear to involve the transfer of two moles of electrons per mole of copper complex as evident from a comparison of the peak currents with those corresponding to the reduction of the mononuclear species. This would mean that the $[Cu^{II}_2L]$ species undergoes a two-electron reduction to $[Cu^{I}_2L]$ which in turn is reduced to $Cu^0$, and that a mixed-valence $[Cu^{II}Cu^{I}L]$ species can be discarded. Although the use of peak currents as a measure of concentration is subject to error, a reasonable correction for the background currents can provide insight into the probable electron stoichiometry of the electrode processes involving the mono- and bi-nuclear species as suggested by the electrochemical parameters in Table 1. To summarize, the electrode reduction of the binuclear species can be described by equations (5) and (6).

$$[Cu^{II}_2H_rL] + 2e^- \longrightarrow [Cu^{I}_2H_rL] \quad (5)$$

$$[Cu^{I}_2H_rL] + 2e^- \longrightarrow 2Cu^0 + 2H_rL \quad (6)$$

Controlled-potential coulometric experiments at potentials intermediate between peaks B and C confirm the foregoing considerations. As Fig. 4(*a*) shows, initial cathodic scan cyclic voltammograms show a progressive decrease of peak B while the CC′ couple remains unchanged. Accordingly, if the scan is started in the anodic direction, the oxidation peak B′, corresponding to the oxidation from $Cu^+$ to $Cu^{2+}$, is initially absent. As shown in Fig. 4(*b*), during the electrolysis peak B′

**Table 2** Frozen-solution (water) ESR parameters for the interaction of $Cu^{2+}$ with ligands $L^1$–$L^3$

| Ligand | $g_{\|}$ | $g_{\perp}$ | $10^4 \lvert A_{\|} \rvert$/$cm^{-1}$ | $g_{\|}/A_{\|}$ |
|---|---|---|---|---|
| $L^1$ | 2.208 | 2.050 | 196 | 113 |
| $L^2$ | 2.202 | 2.050 | 202 | 109 |
| $L^3$ | 2.218 | 2.051 | 194 | 114 |

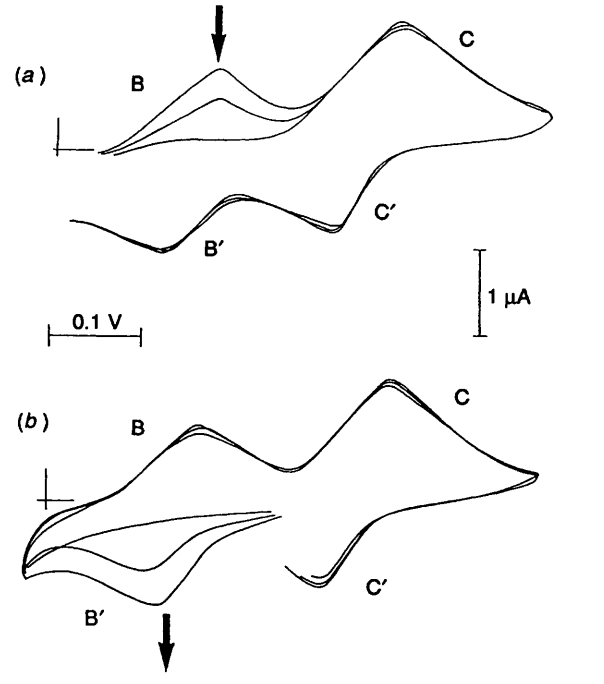


**Fig. 4** Cyclic voltammograms recorded for the controlled-potential electrolysis of a $Cu^{2+}$ (0.80 × $10^{-3}$ mol $dm^{-3}$)–$L^3$ (0.40 × $10^{-3}$ mol $dm^{-3}$) solution at pH 9.0 in 0.15 mol $dm^{-3}$ $NaClO_4$, scan rate 0.05 V $s^{-1}$, initially, at intermediate time and after completion of the one-electron reduction of $Cu^+$. (*a*) Cathodic scan, (*b*) anodic scan

develops, confirming the progressive generation of $Cu^+$. The NMR spectra recorded of the electrolysed solutions in a carefully deaerated argon atmosphere do not show any broadening due to paramagnetic traces and, for instance, the $^{13}C$ NMR spectrum of solutions containing the complex $[Cu^{I}L^1]$ consists of seven sharp signals at δ 30.1, 46.07, 48.2, 50.1, 54.1, 129.7 and 140.1. Moreover, these solutions do not give any significant ESR signal.

On the other hand, ESR spectra of frozen water solutions [or water–methanol (9 : 1 v/v)] of all three $[Cu^{II}L]$ systems recorded at neutral and alkaline pH indicate $CuN_3O$ (or $CuN_2O_2$) chromophores of square-planar geometries (see Table 2). Square-planar $CuN_4$ or $CuO_4$ chromophores give rise

to $g_{\|}$ values around 2.20 and $A_{\|}$ values around 200 × $10^{-4}$ $cm^{-1}$ and therefore for this type of geometry the $g_{\|}/A_{\|}$ ratio is *ca.* 100. In our case the data obtained indicate $CuN_3O$ or $CuN_2O_2$ geometries in which the nitrogen donors will be afforded by the macrocycle and the oxygen atoms will belong to water molecules of the bulk solvent. Occupation of the fifth and sixth co-ordination positions by further N or O atoms, to give 4 + 1 or 4 + 2 tetragonal geometries, can be rejected since this would lead to higher $g_{\|}$ values (around 2.24–2.30) and lower $A_{\|}$ values (less than 180 × $10^{-4}$ $cm^{-1}$).[13]

*Analysis of Complex Formation Equilibria.*—Prior potentiometric studies indicated the formation of mono- and binuclear $Cu^{2+}$ complex species in a pH-dependent stepwise manner.[7,8] The complex formation equilibria can be represented by equation (7), or, alternatively, for the hydroxylated species,

$$mCu^{z+} + nL + rH^+ \longrightarrow [Cu_m(H_rL_n)] \quad (7)$$

by equation (8). In the systems studied $m = 1$ or 2, $n = 1$ and

$$mCu^{z+} + nL + xH_2O \longrightarrow [Cu_mL_n(OH)_x] + xH^+ \quad (8)$$

$x = 1$ or 2. The corresponding cumulative stability constants, $\beta_{mnr}$, have been determined potentiometrically[8] for the different $Cu^{2+}$–ligand systems as well as the cumulative protonation constants, $\beta_j$, for the free ligands [equation (9)]. Hereafter the

$$L + rH \longrightarrow H_rL \quad (9)$$

stability constants for the $Cu^{2+}$ complexes will be labelled as $\beta^{II}_{mnr}$, and the corresponding ones for the $Cu^+$ complexes designed as $\beta^{I}_{mnr}$.

Variation of the electrochemical parameters provides quantitative estimates of the concentration of the complexed metal. For example, Fig. 5 presents the variation of potential and current of cathodic peak A with Cu : $L^1$ molar ratio at pH 5, which clearly suggests the formation of a stable 1 : 1 complex species. A significant decrease in the peak current was observed in all cases.

Variations of the peak current for the anodic peak A′ at the GCE allow the calculation of the mole fraction of uncomplexed copper from the ratio of actual peak intensity to peak intensity in uncomplexed metal solutions. Such values agree closely with those calculated from the distribution diagrams deduced from independent potentiometric data, as depicted in Fig. 3.

On the other hand, application of the generalized molar ratio method[14] enables us to confirm the stoichiometry of the complex species and their conditional stability constants for the process [equations (10) and (11)], providing the mole fraction of

$$mCu^{z+} + nH_rL \longrightarrow [Cu_m(H_rL)_n] \quad (10)$$

$$K = [Cu_m(H_rL)_n]/[Cu^{2+}]^m[H_rL]^n \quad (11)$$

complexed copper is known from cyclic voltammetric data. In a molar ratio experiment, a series of samples containing a constant concentration of $Cu^{2+}$ and varying concentrations of ligand were prepared at constant pH. Only the correct $m$, $n$ stoichiometric coefficients will lead to constancy of the relationship (12), where $c_L$ and $c_M$ are the total concentrations

$$K^* = K^{\frac{1}{n}} = \frac{\alpha^{\frac{1}{n}}}{m^{\frac{1}{n}}(1-\alpha)^{\frac{m}{n}}[c_L - (n/m)\alpha c_M]} \quad (12)$$

of ligand and metal, respectively, and $\alpha$ the mole fraction of complexed copper. Fig. 6 presents plots of $K^*$ *vs.* $\alpha$ for the Cu–$L^1$ system at pH 4.5 at different stoichiometries. A horizontal line is only obtained for a 1 : 1 L : M stoichiometry, the plots being steadily increasing or decreasing for any other stoichiometry. This result confirms the potentiometric data

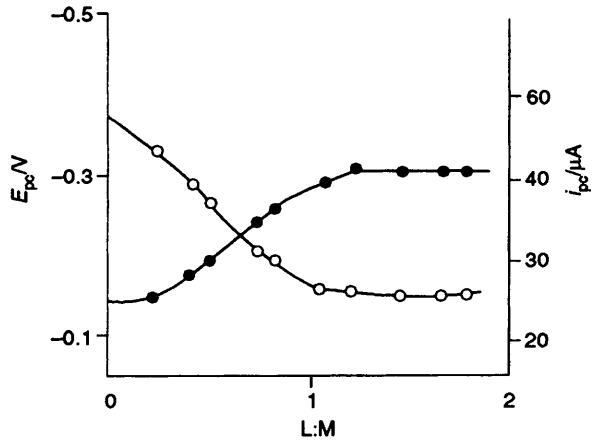


**Fig. 5** Plots of peak potential and peak current for the cathodic process A as a function of L : M ratio for the $Cu^{2+}$–$L^1$ system at pH 5.0. From the cyclic voltammogram at the GCE; scan rate = 0.20 V $s^{-1}$, $c_M$ = 1.58 × $10^{-3}$ mol $dm^{-3}$. Supporting electrolyte 0.15 mol $dm^{-3}$ $NaClO_4$

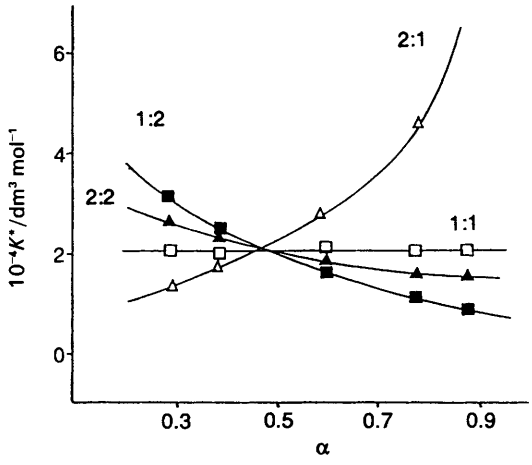


**Fig. 6** Application of the generalized molar ratio method to the Cu–$L^1$ system at pH 4.50. Plots of $K^*$ *vs.* $\alpha$ for different stoichiometries

which indicated that, at weakly acidic pH, only mononuclear complexes exist in solution.

The values of $K$ can be compared with those determined from the stability constants by means of equation (13). The estimated

$$K_{mnr} = \frac{\beta_{mnr}^{\frac{1}{n}}[H]^{\frac{r}{n}}}{c_M^{(1-m)/n}(1 + \Sigma\beta_r[H]^r)} \quad (13)$$

value of $K$ (log $K$ = 4.5) is in agreement with that predicted from the stability constants obtained from the potentiometric data (log $K$ = 4.37). Similar satisfactory results are obtained for all the ligands.

Alternatively, the stability constants $\beta^{II}_{mnr}$ can be evaluated from the shift in the formal potential, $\Delta E(Cu^{2+}$–$Cu^0)$, corresponding to the $Cu^{2+}$–$Cu^0$ couple determined in excess of ligand by means of the well known relationship (14),[15] where

$$\Delta E(Cu^{2+}\text{–}Cu^0) = \frac{2.3RT}{2F} \log \beta^{II}[L][H]^r \quad (14)$$

[L] can be calculated as the ratio $c_L/(1 + \Sigma\beta_r[H]^r)$ from the protonation constants of the ligand determined potentiometrically. The calculated values of $\beta^{II}_{mnr}$ for several complex species are listed in Table 3. Excellent agreement with the values determined from potentiometric data was found in the majority of cases.

**Table 3** Stability constants for the $Cu^{2+}$ and $Cu^{+}$ complexes of $L^1$, $L^2$ and $L^3$ and equilibrium constant for the disproportionation of $Cu^{+}$ species in 0.15 mol $dm^{-3}$ $NaClO_4$ at 298.1 K

| Reaction[a] | $\log \beta^{II}$ | $\log \beta^{II}$ [b] | $\log \beta^{I}$ | $(1/m) \log K'_d$ |
|---|---|---|---|---|
| $Cu + H + L^1 \rightleftharpoons [Cu(HL^1)]$ | 20.823(5)[b,c] | 21.0(4)[d] | 19.7(2)[e] | −2.4(5)[f] |
| $Cu + L^1 \rightleftharpoons [CuL^1]$ | 13.02(1) | 13.0(2) | 11.9(2) | −4.5(5) |
| $Cu + H_2O + L^1 \rightleftharpoons [CuL^1(OH)] + H$ | 3.92(1) | | 2.7(1) | −8.9(3) |
| $Cu + L^2 \rightleftharpoons [CuL^2]$ | 10.41(2)[c,g] | 10.2(2) | 8.8(2) | −1.0(4) |
| $Cu + L^2 + H_2O \rightleftharpoons [CuL^2(OH)] + H$ | 2.27(6) | | 0.4(1) | −6.0(2) |
| $2Cu + L^2 + 2H_2O \rightleftharpoons [Cu_2L^2(OH)_2] + 2H$ | 3.44(3) | | 0.1(1) | −5.9(3) |
| $Cu + L^3 + 2H \rightleftharpoons [Cu(H_2L^3)]$ | 33.28(2)[c,g] | 33.4(5) | 32.4(2) | −5.3(5) |
| $Cu + L^3 + H \rightleftharpoons [Cu(HL^3)]$ | 26.86(4) | 26.1(4) | 25.7(2) | −7.6(5) |
| $Cu + L^3 \rightleftharpoons [CuL^3]$ | 17.73(5) | 18.1(3) | 16.2(2) | −8.4(5) |
| $2Cu + L^3 + H_2O \rightleftharpoons [Cu_2L^3(OH)] + H$ | 16.95(4) | | 12.9(2) | −5.0(5) |
| $2Cu + L^3 + 2H_2O \rightleftharpoons [Cu_2L^3(OH)_2] + 2H$ | 7.50(6) | | 3.2(1) | −6.9(4) |

[a] Charges have been omitted for clarity. [b] From ref. 7. [c] From potentiometric data. [d] Calculated from electrochemical data using equation (14). [e] Calculated from electrochemical data using equation (17). [f] Calculated from electrochemical data using equation (19). [g] From ref. 8.

**Table 4** Formal potentials (V *vs.* SCE) and stability constants for the formation of $[CuL]^{2+}$ and $[CuL]^{+}$ complexes of selected ligands

| Ligand | $E^{0\prime}$ | $\log \beta^{II}$ | $\log \beta^{I}$ |
|---|---|---|---|
| $L^1$ [a] | −0.15 | 13.0 | 11.9 |
| $L^2$ [a] | −0.18 | 10.4 | 8.8 |
| $L^3$ [a] | −0.17 | 17.7 | 16.2 |
| $L^6$ [b] | −0.07 | 17.1 | 17.8 |
| [14]aneN$_4$ [c] | −0.90 | 27.2 | 13.8 |
| [14]aneN$_2$S$_2$ [c] | −0.20 | 15.2 | 13.9 |
| [14]aneS$_4$ [c] | 0.34 | 4.3 | 12.0 |

[a] This work. Values for the stability constants for the formation of copper(II) complexes of $L^{1-3}$ were taken from refs. 7 and 8. [b] Data from ref. 6. [c] Data from ref. 4.

In neutral and alkaline media, the cyclic voltammetric pattern indicates the formation of $Cu^{+}$ species which are stabilized with respect to disproportionation. Then, the Nernstian expression of $E$ for the $Cu^{2+}$–$Cu^{+}$ couple for both the mono- and binuclear species is given by equation (15), or, alternatively, by equation (16).

$$E = E^0(Cu^{2+}\text{–}Cu^{+}) + \frac{2.3RT}{mF} \log\left(\frac{1 + \Sigma K^{I}[H_rL]}{1 + \Sigma K^{II}[H_rL]}\right) \quad (15)$$

$$E = E^0(Cu^{2+}\text{–}Cu^{+}) + \frac{2.3RT}{mF} \log\left(\frac{1 + \Sigma \beta^{I}[L][H]^r}{1 + \Sigma \beta^{II}[L][H]^r}\right) \quad (16)$$

At some intervals of pH, corresponding to the plateaux in Fig. 3, it can be assumed that only one $Cu^{2+}$ and one $Cu^{+}$ complex exist in solution. Under these conditions, the shift in the formal potential of the $Cu^{2+}$–$Cu^{+}$ couple enables us to obtain a direct estimate of the formation constants for the $[Cu^{I}H_rL]$ species providing those for the $[Cu^{II}H_rL]$ species are known [equation (17)]. Equation (17) is also valid for the hydroxylated

$$\log \beta^{I} = \log \beta^{II} + m[E - E^0(Cu^{2+}\text{–}Cu^{+})]/59 \quad \text{(mV at 298 K)} \quad (17)$$

complexes. The values of $\beta^{I}_{mnr}$ calculated from the corresponding $\beta^{II}_{mnr}$ values and the formal potentials are given in Table 3.

Finally, an estimate of the equilibrium constant, $K'_d$, for the disproportionation of the $Cu^{+}$ complex [equation (18)] can

$$2[Cu^{I}_mH_rL] \longrightarrow [Cu^{II}_mH_rL] + mCu^0 + H_rL \quad (18)$$

be calculated from equation (19), where $K_d$ [$\log K_d = 6.24$

$$\log K'_d = \log \beta^{II} - 2 \log \beta^{I} + m \log K_d + \log \beta_r \quad (19)$$

at 298 K, calculated from the electrode potentials for the $Cu^{2+}$–$Cu^0$ (amalgam) (95 mV *vs.* SCE) and $Cu^{2+}$–$Cu^{+}$ (−85 mV *vs.* SCE) couples] represents the equilibrium constant for the disproportionation of $Cu^{+}$(aq) into $Cu^{2+}$(aq) and $Cu^0$(amalgam), and $\beta_r$ is the protonation constant of the $r$-protonated ligand species. For the hydroxylated complexes, equation (20) can be written and equation (19) becomes

$$2[Cu^{I}_mL(OH)_x] \longrightarrow [Cu^{II}_mL(OH)_x] + mCu^0 + L + xOH^- \quad (20)$$

equation (21). The $K'_d$ values estimated from the equilibrium

$$\log K'_d = \log \beta^{II} - 2 \log \beta^{I} + m \log K_d + \log \beta_r + x \log K_w \quad (21)$$

constants and the formal potentials are summarized in Table 3. Decreasing tendency toward disproportionation of $Cu^{+}$ was found in the order $L^3 > L^1 > L^2$.

## Conclusion

Polyazaparacyclophanes $L^1$, $L^2$ and $L^3$ stabilize $Cu^{+}$ towards disproportionation into $Cu^{2+}$ and $Cu^0$. The stability constants reported in Tables 3 and 4 show that this behaviour is reached through lowering the stability of the $Cu^{2+}$ complexes rather than increasing the stability of the $Cu^{+}$ complexes with respect to the analogous copper complexes of the saturated polyazacycloalkanes. For example, it can be seen in Table 4 that the $Cu^{+}$ complex of cyclam[4] displays a stability close to the azaparacyclophanes complexes reported here while its $Cu^{2+}$ complex is much more stable.[16] Somewhat similar behaviour has been reported for a series of mixed saturated thiaazamacrocycles where an increasing number of sulfur donors decreased the interaction with $Cu^{2+}$ rather than increased the interaction with the reduced form.[4] The introduction of sulfur donors seems to be of importance in order to mimic the behaviour of electron-transfer copper proteins like plastocyanine whose active site is based on a tight $N_2S$ co-ordination with another sulfur atom of a methionine residue lying at a much greater distance thereby forming a very distorted tetrahedral geometry.[17] These co-ordination sites define an entatic state[18] and the reduction of $Cu^{2+}$ to $Cu^{+}$ does not produce significant changes in the co-ordination site and geometry of the metal centre. Although the polyazaparacyclophanes reported here do not obviously offer sulfur atoms to the metal centre, they might present a similar minimum rearrangement of the co-ordination site upon co-ordination. Indeed, we have recently shown that $L^1$ co-ordinates to $Cu^{2+}$ through just three out of the four nitrogens present in the macrocyclic framework and presumably $L^2$ co-ordinates through just two nitrogen atoms,[8] the co-ordination spheres being completed by water molecules of the bulk solvent. The

*para*-substituted benzylic moiety prevents the simultaneous co-ordination of both benzylic nitrogens to the same metal cation and $L^2$, for example, even forms binuclear complexes.[8] The ESR spectra for the $Cu^{2+}$ complexes of all three ligands show preferential square-planar co-ordination geometries and, therefore, reduction to $Cu^+$ would possibly imply a change in geometry but no change in co-ordination number. Moreover, in this respect the hydrophobicity afforded by the benzene moiety may also be of importance.[6] These facts may explain why without the presence of sulfur atoms we are getting close to the thermodynamic and electrochemical values reported, for example, for the mixed-donor macrocycle [14]ane$N_2S_2$ (see Table 4). On the other hand, the ligands reported here present a wealth of future developments since we have recently reported[19] that by taking advantage of the asymmetric co-ordination site we can in a number of cases selectively functionalize the benzylic position and in this way, we could, for instance, introduce additional pendant thiol groups to improve the electrochemical approach to the proteins mentioned. Additionally we are modifying either the aromatic spacer or the polyamine bridge to impose steric strains in order to favour more tetrahedral geometries and to analyse how this may affect the electrochemical response of these systems.

## Acknowledgements

We are indebted to the Direccion General de Investigacion Científica y Técnica (PB90-0567) for financial support. One of us (J. F. M.) thanks the Conselleria de Educación i Ciencia for a predoctoral fellowship.

## References

1 R. W. Hay, J. R. Dilworth and K. B. Nolan, *Perspectives on Bioinorganic Chemistry*, JAI Press, London, 1991, vol. 1; O. Farver and I. Pecht, *Coord. Chem. Rev.*, 1989, **84**, 17.
2 L. Siegfried and T. A. Kaden, *Helv. Chim. Acta*, 1984, **67**, 29; K. P. Balakrishnan, T. A. Kaden, L. Siegfried and A. D. Zuberbühler, *Helv. Chim. Acta*, 1984, **67**, 1060; M. J. Martin, J. F. Endicott, L. A. Ochrymowycz and D. R. Rorabacher, *Inorg. Chem.*, 1987, **26**, 3012; D. A. Rocklife and A. E. Martell, *Inorg. Chem.*, 1993, **23**, 3143.
3 Sanaullah K. Kano, R. S. Glass and G. S. Wilson, *J. Am. Chem. Soc.*, 1993, **115**, 592.
4 M. M. Bernardo, M. J. Heeg, R. R. Schroeder, L. A. Ochrymoweycz and D. R. Rorabacher, *Inorg. Chem.*, 1992, **31**, 191.
5 N. Jubran, G. Golub, H. Cohen, Y. Koresh and D. Meyerstein, *J. Chem. Soc., Chem. Commun.*, 1984, 1683.
6 G. Golub, H. Cohen and D. Meyerstein, *J. Chem. Soc., Chem. Commun.*, 1992, 1683.
7 A. Andrés, M. I. Burguete, E. García-España, S. V. Luis, J. F. Miravet and C. Soriano, *J. Chem. Soc., Perkin Trans. 2*, 1993, 749; A. Bencini, M. I. Burguete, E. García-España, S. V. Luis, Juan F. Miravet and C. Soriano, *J. Org. Chem.*, 1993, 4749.
8 A. Andrés, C. Bazzicaluppi, A. Bianchi, E. García-España, S. V. Luis, J. F. Miravet and J. A. Ramírez, *J. Chem. Soc., Dalton Trans.*, 1994, 2995.
9 R. C. Engstrom and V. A. Strasser, *Anal. Chem.*, 1984, **56**, 136.
10 P. Gans, A. Sabatini and A. Vacca, *J. Chem. Soc., Dalton Trans.*, 1985, 1195.
11 M. S. Shuman and I. Shain, *Anal. Chem.*, 1969, **41**, 1818.
12 R. S. Nicholson and I. Shain, *Anal. Chem.*, 1964, **36**, 706.
13 V. Sakaguchi and A. W. Addison, *J. Chem. Soc., Dalton Trans.*, 1979, 600; R. P. Bonomo, I. Riggi and A. J. Di Bilio, *Inorg. Chem.*, 1988, **27**, 2520.
14 A. Beltran, D. Beltrán, A. Cervilla and J. A. Ramírez, *Talanta*, 1983, **30**, 124; A. Bianchi, A. Doménech, E. García-España and S. V. Luis, *Anal. Chem.*, 1993, **65**, 3137.
15 J. Heyrowsky and J. Kuta, *Principles of Polarography*, Academic Press, New York, 1966; D. R. Crow, *Polarography of Metal Complexes*, Academic Press, London, 1970; A. J. Bard and L. R. Faulkner, *Electrochemical Methods*, Wiley, New York, 1980.
16 M. Kodama and E. Kimura, *J. Chem. Soc., Dalton Trans.*, 1977, 1473.
17 J. M. Guus and H. C. Freeman, *J. Mol. Biol.*, 1983, **169**, 521; J. M. Guus, P. R. Harrowell, M. Murata, V. A. Norris and H. C. Freeman, *J. Mol. Biol.*, 1986, **182**, 361.
18 B. L. Vallee and R. J. P. Williams, *Proc. Natl. Acad. Sci. USA*, 1968, **59**, 498.
19 M. I. Burguete, B. Escuder, E. García-España, S. V. Luis and J. F. Miravet, *Tetrahedron Lett.*, 1994, **35**, 9075.

*Received* 24*th June* 1994; *Paper* 4/03839H